THE ASTROPHYSICAL JOURNAL, 446:250–260, 1995 June 10

ON SPECTRAL LINE FORMATION AND MEASUREMENT IN CEPHEIDS: IMPLICATIONS TO DISTANCE DETERMINATION

C. N. SABBEY,[1,2] D. D. SASSELOV,[1,3,4] M. S. FIELDUS,[5] J. B. LESTER,[3,6] K. A. VENN,[7] AND R. P. BUTLER[8,9]

Received 1994 August 11; accepted 1994 December 20

ABSTRACT

The formation and measurement of Cepheid photospheric spectral lines are explored to understand better the systematic effects involved in radial and pulsation velocity determination, and hence to help secure Cepheid distance scale calibrations that depend on Cepheid velocities (e.g., the Baade-Wesselink method). Using high-resolution optical and infrared spectra and synthetic line profiles, we examine techniques for measuring the position of line center and the amount of asymmetry of Cepheid absorption line profiles. The line asymmetry is observed to be a specific function of pulsation phase and to correlate with line center measurements, thus (1) the conversion factor between radial and pulsation velocity (p-factor) may not be assumed constant with phase and (2) there is a systematic offset of about 1 km s^{-1} in the center-of-mass velocity. Our Cepheid models, which employ non-LTE radiative hydrodynamics, reproduce and describe (as an opacity effect) the observed unequal line asymmetry magnitudes during contraction and expansion stages. The models also allow us to study the phase dependence of the p-factor and its influence on Baade-Wesselink radius calculations. We conclude that in order to reach an accuracy of better than 7% (0.15 mag) in the zero point of the Cepheid distance scale, these systematic effects should be taken into account.

Subject headings: Cepheids — line: formation — line: profiles — stars: distances — techniques: radial velocities

1. INTRODUCTION

Cepheid variable stars have been used as distance indicators, via the celebrated period-luminosity relation, for more than seven decades (indeed, they were the basis for Hubble's extragalactic distance scale), and they have emerged today as the most accurate primary distance indicator (Jacoby et al. 1992). The Baade-Wesselink (BW) method of determining the mean radius of a pulsating star (Baade 1926; Wesselink 1946), due to its solid basis on first principles and adequate Cepheid sample size, has served, since its inception, as one of the primary means for setting the zero point of the Cepheid period-luminosity relation (Walker 1988 describes five additional approaches). Despite this reassuring state of affairs (Gieren, Barnes, & Moffett 1993; Welch 1994), several obstacles remain to be addressed in order to reach an accuracy of 5% with the BW method.

Gautschy (1987) provides an in-depth review of the BW method and a general outline of the uncertainties involved; our paper will focus only on the Cepheid radial velocity measurement and its conversion to pulsational velocity. An understanding of these errors is crucial not only for the BW method and its variants (e.g., the Barnes-Evans method, Barnes & Evans 1976), but also for interferometry techniques that should be feasible in the near future. With the arrival of the next generation of stellar interferometers (such as the Sydney University Stellar Interferometer, Davis 1994), it will be possible to measure Cepheid radii by combining interferometrically measured angular diameter variation with the spectroscopically determined pulsation velocity curve, demanding accurate pulsation velocities.

An understanding of spectral line formation and measurement is central to our discussion. Classical Cepheids are supergiants of moderate effective temperature with fairly broad photospheric absorption lines due mainly to pressure and Doppler broadening. Although their rotational velocities (with upper limits typically <10 km s^{-1}, e.g., see Breitfellner & Gillet 1994) are not large enough to alter noticeably the absorption profiles, a variety of effects contribute to spectral line asymmetries associated with the radial pulsation of the Cepheids (see § 2.2). These phase-dependent asymmetries, of magnitude roughly 20%–40% of the pulsational Doppler shift of the lines, are well documented observationally (Schwarzschild, Schwarzschild, & Evans 1948; van Hoof & Deurinck 1952; Sanford 1956; Bell & Rodgers 1964; van Paradijs 1971; Sasselov & Lester 1990; Albrow & Cottrell 1993, 1994; Butler 1993).

Variably asymmetric absorption profiles with widths comparable to the pulsation Dopper shift can result in significant systematic errors in radial velocity measurement. Section 2.3 will discuss this roughly 5%–10% effect on the BW radius (and ultimately distance) solution. Also, the center-of-mass velocity of a Cepheid (as derived from its radial velocity curve) will be in error with a similar effect on the BW radius. Section 4 deals with this approximately 5%–10% effect.

In addition to the influence of line asymmetry on radial velocity measurement, there are systematic effects intrinsic to

[1] Harvard-Smithsonian Center for Astrophysics, 60 Garden Street, Cambridge, MA 02138; sabbey@cfassp.harvard.edu, sasselov@cfa.harvard.edu.
[2] Yale University, Department of Astronomy, P.O. Box 208101, New Haven, CT 06520-8101; sabbey@astro.yale.edu.
[3] Visiting Astronomer, Canada-France-Hawaii Telescope, operated by the NRC of Canada, the CNRS of France, and the University of Hawaii.
[4] Hubble Fellow.
[5] Department of Astronomy, University of Toronto, Toronto, Canada; Deceased 1992 July 3.
[6] Department of Astronomy, Erindale College, University of Toronto, Mississauga, ON, Canada L5L 1C6; lester@astro.utoronto.ca.
[7] University of Texas, Department of Astronomy, RLM 15.308, Austin, TX 78712; and Institüt für Astronomie, Univ. Sternwarte-München Scheinerstr. 1, 81925 Munich, Germany; venn@hal2.usm.uni-muenchen.de.
[8] Astronomy Department, University of California, Berkeley, CA 94720; paul@further.berkeley.edu.
[9] Department of Physics and Astronomy, San Francisco State University, San Francisco, CA 94132.

the star that must be taken into account when converting from radial to pulsational velocity. The factor of this conversion ($p \equiv V_{\rm pulsation}/V_{\rm radial}$) will not be constant. Although it has been noted (e.g., Gautschy 1987) that the p-factor should be a function of phase, only constant p-factors have been applied to date. Section 4 deals with this roughly 5% effect.

The study of how atmospheric pulsation influences absorption profiles and the p-factor is certainly not new—just 5 years after Shapley first postulated cyclic pulsation to explain Cepheid variability, Shapley & Nicholson (1919) established the theoretical profile of an absorption line produced in an outward or inward moving stellar atmosphere. This work was extended by Carroll (1928), Getting (1935), Underhill (1947), Parsons (1972), Karp (1975a, b), Hindsley & Bell (1986), Albrow & Cottrell (1994), and others. The additional insights in the present work are based on a combination of recent high-quality spectral observations and on theoretical absorption profiles produced by our calculations with the code HERMES (Sasselov & Raga 1992), which employs non-LTE radiative hydrodynamics.

2. OBSERVED ABSORPTION LINE PROFILES

2.1. *The Data*

The Cepheids chosen for this study are δ Cephei, η Aquilae, ζ Geminorum, and X Sagittarii. They are standard classical Cepheids that have been monitored for many years; it is unlikely that they are peculiar members of their class. Optical and infrared spectra have been obtained.

The high-resolution ($R = \lambda/\Delta\lambda \approx 30{,}000$) infrared spectra of the Cepheids η Aql, X Sgr, and ζ Gem, were taken by Sasselov & Lester (1990, and references therein) with the Fourier Transform Spectrometer (FTS) at the Canada-France-Hawaii Telescope (CFHT) in 1988 April, September, and October and 1989 March. Moderately full phase coverage of each star was obtained (a total of 25 spectra), in the spectral region centered near 1.1 μm (with a bandwidth of approximately 350 Å). A thorough description of the FTS can be found in Maillard & Michel (1982), while information concerning the measurement of the spectra can be obtained in Sasselov & Lester (1990). Simultaneous high-resolution optical spectra of the Cepheid ζ Gem were taken at the McDonald Observatory (by M. S. F. and K. A. V.) using the 2.1 m telescope and a coudé reticon camera. The 11 spectra (shown in Fig. 1), centered on 6560 Å with a bandwidth of 100 Å, provide moderate phase coverage.

The high-resolution ($R \approx 40{,}000$) optical spectra of the Cepheids δ Cep and η Aql were obtained by R. P. B. in 1990 August at the Lick Observatory with the 0.6 m Coudé Auxiliary Telescope and the "Hamilton" spectrograph, a cross-dispersed coudé echelle spectrometer equipped with a TI 800 × 800 CCD. Full-phase coverage of both stars was obtained (a total of 21 spectra), with each spectrum (centered on ≈5600 Å) capturing 50 dispersion orders (each 40 Å long), leaving ≈20 Å between orders undetected. For a complete description of the instrument and procedure used to measure the spectra, see Butler (1993), and references therein.

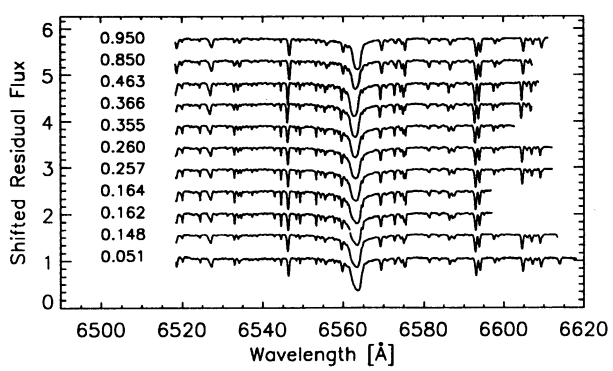

FIG. 1.—McDonald Observatory spectra of ζ Gem in the Hα region

Table 1 lists the absorption lines chosen for our study. There is ample reason to be confident that the results are not significantly contaminated by line blending effects. Spectral syntheses kindly provided by R. Kurucz (1994, private communication) have been examined to detect hidden blends, and the shapes of the line asymmetries were similar for different absorption profiles at the same pulsation phase. In addition, there is substantial evidence insuring us that the line asymmetries studied are not artifacts of the instrument or reduction procedure. Inspection of the telluric lines (which remain symmetric) and the consistency of results taken with different instruments at different times provide strong confidence—for further discussion of this issue, see Sasselov & Lester (1990).

2.2. *Measuring Line Asymmetry*

As will be shown, absorption line asymmetry systematically offsets measurements of line center by an amount dependent

TABLE 1

ABSORPTION LINES USED

Ion	λ (Å)	X Sgr	η Aql	ζ Gem	δ Cep
Fe I.....	5135.11	...	x	...	x
Mg I.....	5174.14	...	x	...	x
Ti II	5187.35	...	x	...	x
Fe II.....	5199.02	...	x	...	x
Sc II	5241.28	...	x	...	x
Fe I.....	5283.27	...	x	...	x
Sc II	5319.83	...	x	...	x
Fe I.....	5325.66	...	x	...	x
Ti II	5338.30	...	x	...	x
Fe II.....	5339.21	...	x	...	x
Fe I.....	5342.52	...	x	...	x
Fe I.....	5368.95	...	x	...	x
Fe I.....	5375.20	...	x	...	x
Fe I.....	5384.87	...	x	...	x
Fe I.....	5390.98	...	x	...	x
Fe I.....	5392.97	...	x	...	x
Fe I.....	5394.67	...	x	...	x
Ti II	5420.29	...	x	...	x
Sc II	5528.36	...	x	...	x
Mg I.....	5530.00	...	x	...	x
Fe I.....	5817.97	...	x	...	x
Fe I.....	5936.31	...	x	...	x
Fe I.....	6004.69	...	x	...	x
Fe I.....	6057.67	...	x	...	x
Si I	6126.72	...	x	...	x
Si I	6146.72	...	x	...	x
Si II.....	6348.86	...	x	...	x
Fe I.....	6546.25	...	...	x	...
Ti II	6559.58	...	...	x	...
Fe I.....	6569.26	...	...	x	...
C I.....	10683.09	x	x	x	...
C I.....	10685.34	x	x	x	...
Si I	10694.25	x	x	x	...
C I.....	10707.32	x	x	x	...
Si I	10727.41	x	x	x	...
C I.....	10729.53	x	x	x	...
Si I	10749.38	x	x	x	...
Si I	10784.56	x	x	x	...
Si I	10786.85	x	x	x	...
Si I	10843.86	x	x	x	...

on the method of measuring line center *and* the magnitude of the asymmetry. Thus, in acquiring radial velocities by line center measurements we must understand the sources of the observed profile asymmetry as well as the sensitivity of our technique for measuring line center. Sources of profile asymmetry are discussed in § 3.2. In the next section we discuss the change in *p*-factor required for different methods of measuring line center. Below we describe how asymmetry magnitude was measured.

Cepheid line asymmetry has been previously quantified by the difference or quotient of the red and blue half-widths of the absorption profile at half-depth (see Ciurla 1966; van Paradijs 1971; Sasselov & Lester 1990; Butler 1993), and by examination of the spread of line center measurements obtained using line bisectors at depths of 0.5–0.9 (Wallerstein et al. 1992; Albrow & Cotterell 1994). An extension of these techniques has been employed here in order to sample fully the absorption profile. An asymmetry percentage for each absorption line was determined from the difference and sum of the areas of the red and blue profile halves: $(A_{red} - A_{blue})/(A_{total}) \times 100$. A parabola fit to the core is used to determine line center. The method successfully quantifies what we observe by eye. An example of this method of asymmetry measurement is provided in Figure 2. By using the entire profile for measuring asymmetry, we reduce the scatter in the asymmetry plot and avoid possible systematic errors (e.g., at some phases the asymmetry is prevalent between continuum and half-depth). Note that the dashed line in Figure 2 is 2% below the stellar continuum; it is set by eye as judged by the signal-to-noise ratio in our data and minimizes the introduction of noise into the asymmetry measurements. The line asymmetry results were found to be insensitive to the exact placement of this upper bound.

The measured asymmetries as a function of phase (as well as line center measurements to be discussed in the next section) are presented in Figure 3. The amplitudes of the asymmetry curves increase with pulsation velocity amplitude, and they are roughly the magnitude expected from the projection effect. An exception is the X Sgr spectra which had asymmetries several times greater than expected by the projection effect alone, although this can be attributed to the line splitting present in these spectra.

Perusal of the asymmetry curves yields considerable insight into the pulsation dynamics of the program Cepheids—although the general shape of the asymmetry curve is dominated by the projection effect, there are features deserving further study. For example, the absorption profiles for every Cepheid studied, in both wavelength regions, exhibited greater asymmetry magnitudes during contraction than during expansion. This confirms the discrepant line asymmetries measured earlier by Sasselov & Lester (1990), Butler (1993), and Albrow & Cottrell (1994). (It should be noted however, that this discrepant asymmetry is observed in all standard photospheric lines in Butler's 1993 study, but not for the small group of low-excitation-potential lines.) Also, although the optical and infrared lines of η Aql attain about 15% asymmetry at maximum in the contraction speed, the asymmetry at maximum expansion differs by a factor of 2 (see Fig. 4). In this paper we add to the previous results a comparison between the simultaneous infrared and optical data for ζ Gem (which exhibits a similar disparity).

In addition to serving as a diagnostic tool for characterizing atmospheric dynamics, the shape of the asymmetry curve also explains systematic errors involved in velocity measurement

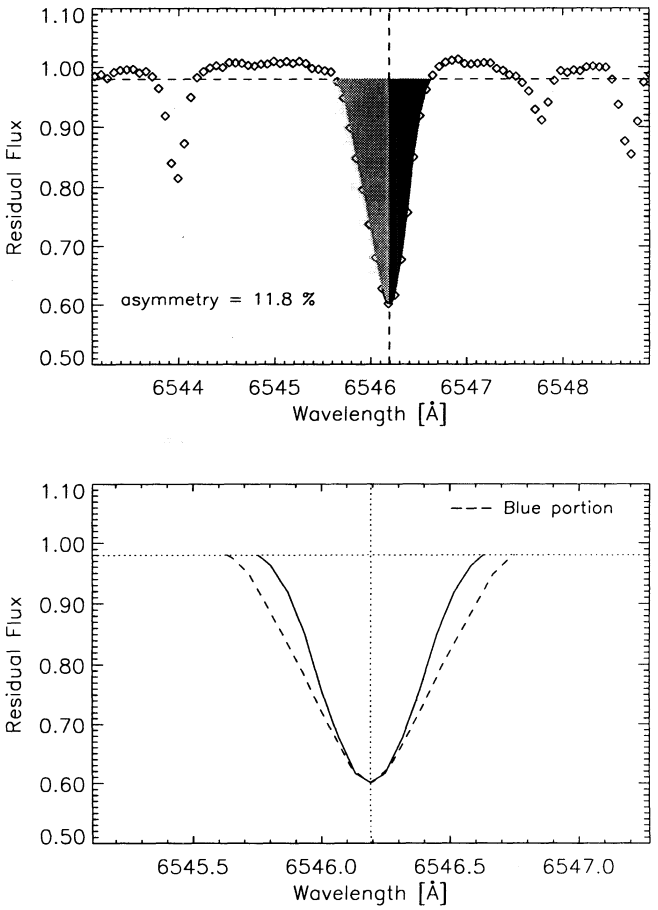

FIG. 2.—Example of the method for measuring line asymmetry. The asymmetry is emphasized in the bottom plot by flipping each profile half to obtain a whole profile and overplotting the results (there was no instance in which the new profiles were interwoven, yielding an inaccurate measurement of asymmetry).

(discussed in the next section), and suggests a possible solution to the Cepheid K-term problem (§ 4.1).

2.3. *Measuring Line Center*

The particular method employed in measuring the Doppler shift of photospheric absorption lines is crucial—different methods yield systematically different results. The two methods of measuring line center to be discussed are (1) the parabola method, that is, determining the center of a parabola fit to the line core, and (2) the line bisector method, which consists of finding the midpoint between the red and blue wings of the profile at a given depth, such as the half-depth used here. The advantage of contrasting the results of these two methods is that they represent the extremes in sensitivity to profile shape. For example, Gaussian fits to the profiles (as well as line bisectors between half-depth and profile minimum) consistently yielded line centers between those derived from the parabolic fit to the line core and from the half-depth line bisector. Line bisectors are not obtained for depths between continuum and half-depth due to susceptibility to noise and blends with weak lines.

For perfectly symmetric line profiles, the parabolic and line bisector methods of determining line center will agree; for the

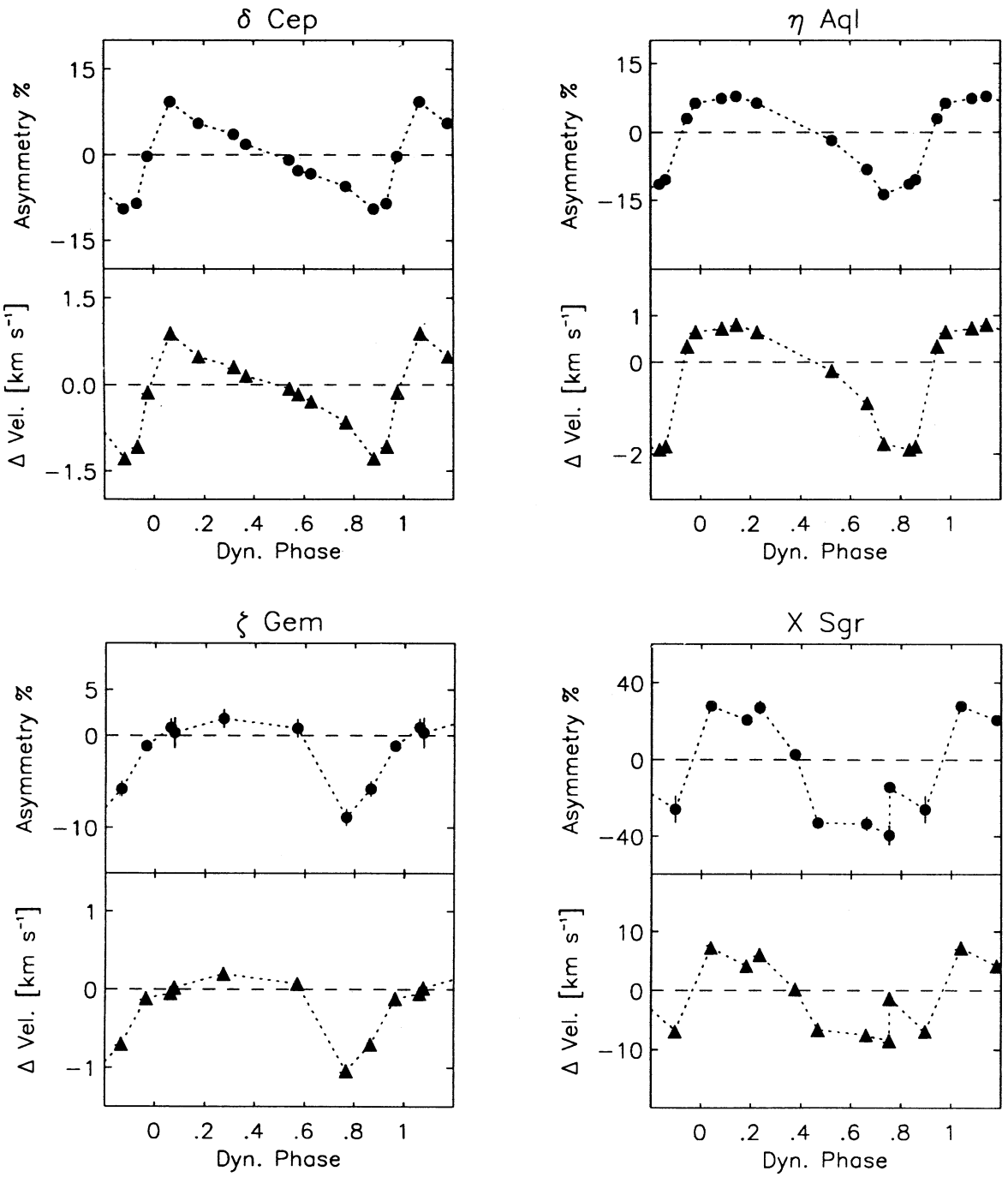

FIG. 3.—Line asymmetries of the observed lines and the corresponding measured velocity discrepancy between the parabola and line bisector methods of measuring line center. The x-axis has been labeled with the dynamical phase of the Cepheid (dynamical phase 0.0 is marked by the occurrence of the velocity reversal from contraction to expansion of the photosphere). The asymmetries are in the direction of zero Doppler shift, as we would expect if the projection effect dominates the observed line asymmetry. The disagreement between different methods of measuring line center is a systematic effect dependent on the magnitude of line asymmetry. The line bisector method is more sensitive to line asymmetry than the parabola method (which samples the line core); the p-factor for the line bisector method will be about 5% larger than for the parabola.

preponderance of Cepheid absorption profiles, which are asymmetric, the methods will provide divergent results. Figure 3 presents the velocity differences between parabolic and line bisector measurements of line center as a function of phase for each program Cepheid. The correlation between line asymmetry and discrepancy between the two methods applied to measure line center is remarkable. Unless the p-factor is determined for the particular method applied to measure line center, the result is a significant systematic error (of roughly 5%–10% of the velocity amplitude, and for X Sgr, roughly 30%).

It is clear that there is no consensus regarding the proper method for determining line center, but what compounds the problem is that some authors have often neglected to discuss or even mention their choice. In recent years, however,

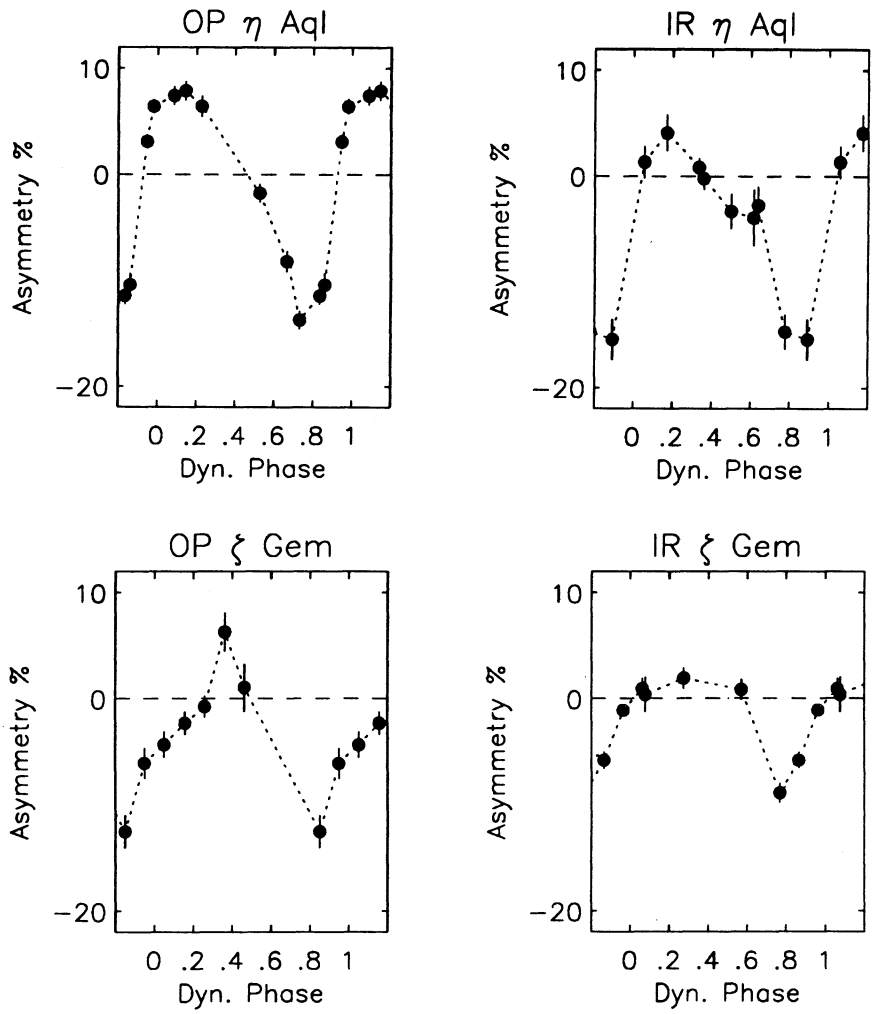

FIG. 4.—Absorption line asymmetry curves for the optical and infrared data of η Aql and ζ Gem. Although each Cepheid exhibits a similar asymmetry magnitude in the two wavelength regions near maximum contraction speed, the asymmetry near maximum expansion speed differs by about a factor 2 between wavelength regions.

increased attention has been given to the discussion of a suitable method for measuring line center (*e.g.*, Albrow & Cottrell 1993; Wallerstein et al. 1992; Butler 1993). Although problems with both methods exist (e.g., the line bisector result can depend greatly on the depth chosen, see Fig. 5), the important point is to use a *p*-factor that reflects the technique used to measure line center.

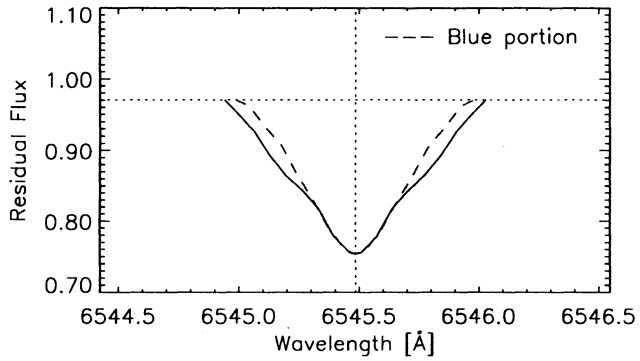

FIG. 5.—Same as Fig. 2 (*lower panel*), but for a spectral line with a complex asymmetry profile. A problem with using the line bisector method to measure line center is that the result can depend significantly on the exact depth chosen; Wallerstein et al (1992) confront this difficulty by applying the line bisector over a range of line profile depths for each measurement of line center.

3. THEORETICAL LINE PROFILES

Cepheids are distant point sources, and we cannot study center-to-limb variation in their spectral line profiles. In addition, we have very marginal depth resolution, because the line-forming regions of the photospheric lines are closely spaced and overlapped. The shape of a photospheric absorption line profile is a complicated function of the temperature and pressure structure of the atmosphere, the motions of the atmosphere (including macroturbulence, microturbulence, pulsation, velocity gradients, and shock waves), and the intensity-weighted projection effect. Due to this complex mapping and degeneracy in parameter space, it is not possible to study the systematics related to the time-dependent atmospheric structure on an empirical basis alone. Hence both the projection factor and any systematic errors in the γ-velocity must be determined theoretically.

3.1. *The Models*

Dynamic Cepheid atmospheres have been computed by a number of people, but the most recent serious effort was by Karp (1975a, b). All these models are dynamic, but in plane-parallel geometry and with gray atmospheres. Their low-order hydrodynamic schemes, with artificial viscosity, have prevented quantitative radiative transfer calculations (the main reasons have been outlined by Hilendahl 1968, p. 105; and Mihalas & Mihalas 1984, p. 287). Therefore, the best synthetic line profiles for Cepheids based on "snapshots" from a first-order hydrodynamic calculation are from LTE atmospheres with a modified version of the ATLAS code (Albrow & Cottrell 1993; Albrow 1994). These have constant micro- and macro-turbulence parameters which are arbitrary. In addition, the first-order hydrodynamic Cepheid model represents the time-dependent dynamic atmosphere adequately only on the average. While the work of Albrow & Cottrell (1993, 1994) is a major achievement in the study of Cepheid atmospheres, a coupled non-equilibrium calculation is needed for the time-dependent systematic effects, which we have set forth to study in this paper.

We have calculated hydrodynamic non-LTE models of Cepheid atmospheres with the code HERMES of Sasselov & Raga (1992). The non-LTE radiative transfer solver is based on the program MULTI by Carlsson (1986), updated with an improved treatment of background opacities based on Gustafsson et al. (1975). The hydrodynamic calculation is based on a stable second-order scheme, without artificial viscosity to stabilize the solutions. The depth-dependent nonthermal broadening is computed consistently within the scheme, instead of assigning the ad hoc micro and macroturbulence parameters. This is important for synthesizing realistic Cepheid line profiles, but also because microturbulence, that is, velocity fields on scales small compared to a photon mean-free-path, can reduce the gas pressure contribution and thus the opacity. The heating and cooling from H, Ca II, and Mg II is treated in a detailed multilevel non-LTE manner. Additional details about the dynamic models are in Sasselov & Lester (1994).

The model output provides complete time-dependent information about the line formation of a large number of spectral lines. Throughout this paper we shall use for illustration our model for the Cepheid ζ Gem and the photospheric lines of Mg II ($4s\,^2S$–$4p\,^2P$) at 9226.9 Å and Mg II ($3d\,^2D_{5/2}$–$4p\,^2P_{1/2}$) at 10951.8 Å; the latter line is present in our infrared spectra of ζ Gem (see Fig. 6).

The determination of the depth of formation of spectral lines will be accomplished through the use of a contribution function (CF), which gives the relative contribution of the different layers to the observed quantity. Here we define (see Magain 1986) the contribution function, CF, for the relative line depression, as

$$\mathrm{CF}(\log \tau_0) = \frac{\log 10}{\mu}\,\tau_0\,\frac{\kappa_l}{\kappa_0}\left(1-\frac{S_l}{I_c}\right)e^{-\tau_R/\mu},$$

where τ_0 is the optical depth at a reference wavelength λ_0, τ_R is defined in terms of $\kappa_R = \kappa_l + \kappa_c S_c/I_c$, κ_0 is the absorption coefficient at λ_0, κ_l and κ_c are the line and continuum absorptions, respectively, S_l and S_c are the line and continuum source functions, respectively, I_c is the emergent continuous intensity (if the line were absent), and $\mu = \cos\theta$. The traditional dependence on frequency has been omitted from our notation for simplicity. The CF for a given synthesized spectral line will indicate where the line is formed, that is, the line-forming region, and consequently, at what velocity. For the comparison with our observations, we have used a CF which accounts for the contribution from the underlying continuum.

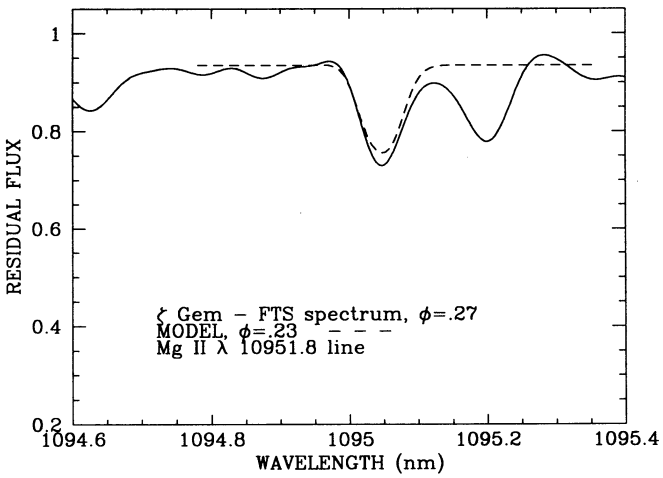

FIG. 6.—Spectral line of Mg II λ10952, observed and synthesized in ζ Gem and its dynamic non-LTE model at about phase 0.25.

3.2. *The Line-Forming Region as a Function of Phase and the Line Asymmetry Curve*

In Cepheids most photospheric lines are formed under conditions close to LTE; *however*, these local conditions are determined (at each moment) by a dynamic atmosphere which is neither in hydrostatic nor in radiative equilibrium (Willson 1988; Sasselov & Lester 1994). This has the effect of complicating a line's contribution function (in velocity vs. atmospheric depth parameter space), due to the extension of the line-forming region outwards (in depth). An example is given in Figure 7, which demonstrates the much thinner (in depth) line-forming region in an equilibrium atmosphere. Consequently, velocity gradients and other depth-dependent perturbations are not likely to have a noticeable effect on synthetic line profiles from equilibrium calculations.

As can be seen in the upper panel of Figure 7, the line's CF is generally of a complex form. If the pulsation led to a coherent rising and falling of the atmosphere, then this complexity of the CF would be practically time-independent. Thus, the only effect on the emergent line profile would be depth-dependent thermal broadening, which could be safely ignored as compared to the much more significant change of the absorption line strength due to the general temperature and density variation of the coherent atmosphere. However, the concept of a coherently pulsating atmosphere is not supported by the observations of Cepheid and is not justified theoretically. In other words, substantial velocity gradients are present throughout a Cepheid atmosphere in all hydrodynamical models. For the longer-period (and larger-amplitude) Cepheids, these often evolve into discontinuities (shock waves).

The main effect that velocity gradients have on photospheric line profiles is to introduce time-dependent asymmetries. This corresponds to a broadening of the line's CF profile in the velocity versus depth plane. Shock waves can disrupt the CF profile, with the result that the emergent line profile is a superposition of Doppler-shifted components (each with their differ-

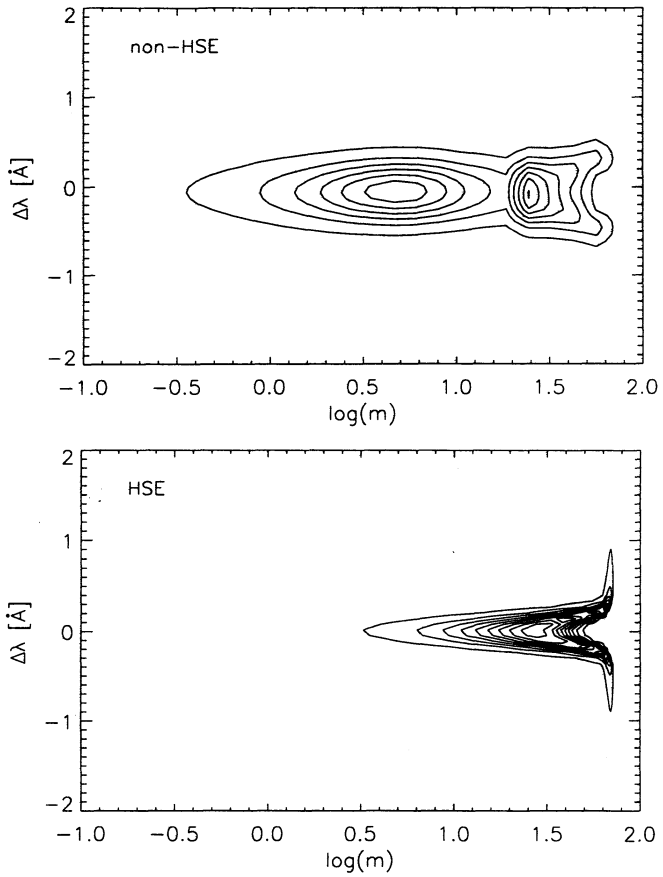

FIG. 7.—Contribution function of the Mg II λ10952 line in units of intensity (ergs cm^{-2} s^{-1} Hz^{-1} sr^{-1}). The contours are in logarithmic scale. Atmospheric depth (x-axis) is given in terms of column mass (*m*). The same non-LTE calculation was performed for the hydrostatic equilibrium (HSE) atmosphere, which corresponds to the "snapshot" photospheric parameters at $\phi = 0.55$ of the dynamic ζ Gem model.

ent strength and asymmetric profile). Fortunately, in classical Cepheids strong shock waves seem rarely to be present in the photosphere, and only for a very short time if they are present. On the other hand, velocity gradients, being long-lived and subtle, could seriously affect the Doppler shifts derived from the spectral lines. In order to study these effects, we shall use our synthesized line profiles and measure their Doppler shifts and asymmetries in the same manner we did for the observed data in § 2. Then we shall compare the synthetic (or theoretical) radial velocity curves to the actual (also theoretical) motion of the photosphere and the corresponding line-forming regions.

We determine the velocity of the volume of gas producing a given spectral line with the help of the line's CF. More specifically, at each model phase we determine the average optical depth of line formation by doing a contributed-weighted average of optical depth, τ, over all τ-frequency bins in the two-dimensional contribution function, and then interpolate the velocity at that depth in the model atmosphere velocity field. The precision provided by the representative τ was about 0.3 km s^{-1}. By deriving the pulsation velocity using this method, and obtaining the simulated radial velocity by measuring the Dopper shift of the theoretical absorption profiles, we are able to study the phase dependence of the *p*-factor and its influence on Baade-Wesselink radii (§ 4).

We also obtained a theoretical line asymmetry curve which can be compared to our observed line asymmetry curve of ζ Gem at 1.1 μm in Figure 8. The success of the model in reproducing both the amount and the phase-dependent pattern of the line asymmetry is striking, despite the deviation near phase 0.95. The particular shape of the theoretical asymmetry curve is a very robust result (easily reproducible for any photospheric line), which has a readily identifiable source—the depth variation of the line-forming regions with phase seen in Figure 9 (Plate 9).

4. THE γ-VELOCITY, VARIABLE *p* FACTOR, AND BAADE-WESSELINK RADII

4.1. *Systematics in the γ-Velocity*

The observed unequal line asymmetry magnitudes during contraction and expansion are due to the varying depth of spectral line formation over a Cepheid pulsation cycle. In other words, the photospheric spectral lines in a Cepheid atmosphere are not associated with the same gas particles during a cycle. Therefore, they are not required to, and indeed do not, comply with *path conservation*

$$\int v_{\rm rad}\, d\phi = 0\,,$$

where the integral is over a complete Cepheid cycle. However,

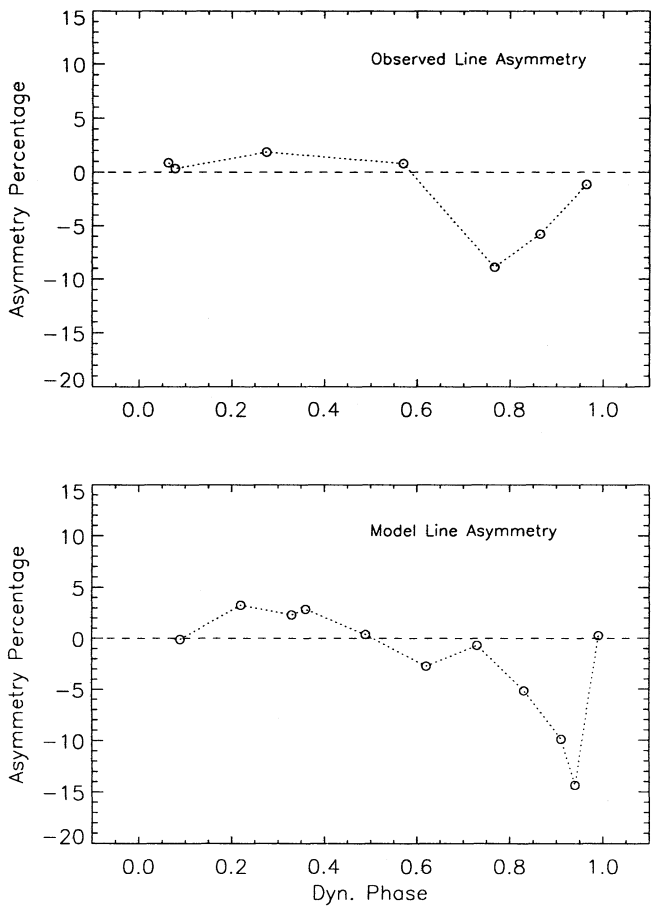

FIG. 8.—Line asymmetry measured from the infrared ζ Gem spectra and from the hydrodynamic non-LTE model lines.

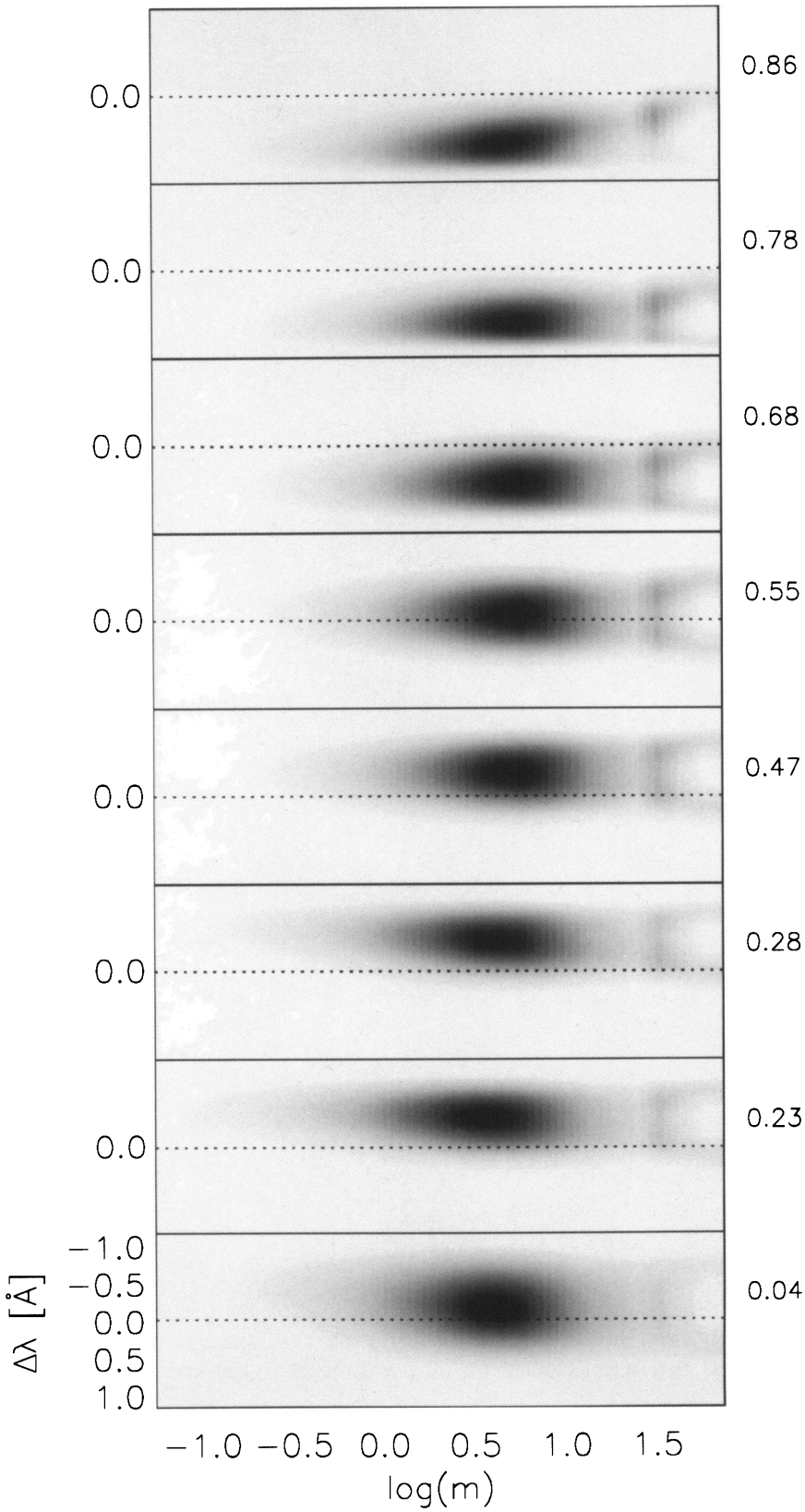

FIG. 9.—CFs of the photospheric Mg II line in the ζ Gem model are shown over the full cycle. Atmospheric depth (x-axis) is given in terms of column mass (m); pulsation phases are marked on the right. The depth variation is clearly visible, in addition to the changes in the extent of the line-forming region, as represented by the CF.

SABBEY et al. (see 446, 256)

path conservation is a basic assumption in the BW method (Gautschy 1987). Path conservation is used to derive the center-of-mass velocity (commonly referred to as γ-velocity) of a pulsating star from the above integral of the observed radial velocity. Based on the consistently unequal asymmetry magnitudes during contraction and expansion for every Cepheid studied (see Figs. 3 and 4), we would expect an average error in γ-velocity determinations of roughly 1 km s^{-1} toward us (Doppler blueshift). The systematic velocity effect is illustrated in Figure 3; the larger line asymmetry during phases of contraction leads to underestimating the measured velocities, as opposed to the phases of expansion, resulting in an overall systematic offset.

It is tantalizing that observational evidence along these lines has been available for more than 40 years (Parenago 1947; Stibbs 1956; Wielen 1974). In these studies of the kinematical behavior of Cepheids in our vicinity of the Galaxy, they found that the Cepheids show a "K-term" (a residual line-of-sight velocity) in their radial velocities of the order of -2 km s^{-1} (toward us). New, more accurate velocity observations of Cepheids confirm the reality of the K-term problem (Caldwell & Coulson 1987; Wilson et al. 1991; Barnes 1993, private communication; Pont, Mayor, & Burki 1994).

Wielen (1974) found no correlation of the K-term with any obvious parameter, like period, amplitude, or distance, and concluded that the K-term is an intrinsic property of Cepheid atmospheres. On the other hand, Pont et al. (1994) try to revive Parenago's (1947) suggestion, that the K-term is due to a real effect in the dynamics of the galaxy. The best way to solve the problem would be a detailed radial-velocity comparison of cluster Cepheids with their early-type neighbors (as originally suggested by M. W. Feast). Current data for such comparison (used by Pont et al. 1994) come from studies to establish cluster membership (Mermilliod, Mayor, & Burki 1987; Harris et al. 1987), which is not sufficient to solve the K-term problem.

The result here suggests that a possible solution to the K-term problem may indeed be found in terms of an atmospheric phenomenon—the varying depth of the photospheric line-forming region with phase.

4.2. *The Projection Factor as a Function of Pulsation Phase*

For numerous reasons, measurement of the Doppler shift of photospheric absorption line profiles does not directly yield a pulsation velocity representative of the continuum forming region (which is crucial for the consistent application of the BW method). The most obvious deviation is introduced by the "projection effect," which is simply the result of observing a weighted mean of the varying line-of-sight component of the pulsation velocity across the disk. For a sphere expanding and contracting in a radial fashion, the observed velocity, $V_{\rm obs}$, will be linearly related to the pulsation velocity of the sphere: $V_{\rm puls} = pV_{\rm obs}$. The observed velocity is often referred to as radial velocity, $V_{\rm radial}$, in the literature as well as throughout this paper. The projection factor ("p-factor"), usually ≈ 1.4, is determined by geometry and the expected intensity contribution as a function of surface position (e.g., cool stars have limb darkening that requires that more weight is given to disk center velocities).

The theoretical argument that p is not a constant (with phase) is based on the fact that the disk-integrated line profiles depend on the limb darkening and line broadening, which vary with phase due to the radial pulsation (and a temperature range of 1000 K or more). However, the first empirical evidence which points strongly to the significance of these effects is the variation of the Cepheid line asymmetry curves presented and interpreted in this paper (§§ 2–3). Moreover, the consistently greater line asymmetry observed during contraction phases suggests a systematic effect independent of pulsation period (luminosity). The inequality of contraction and expansion in terms of photospheric line formation, evident in the differing line asymmetries, already invalidates the underlying BW assumption of coherent or homologous motions in the atmosphere (see Gautschy 1987). Note that this assumption was not challenged in the studies of the dependence of the p-factor on limb darkening, velocity, line strength (Parsons 1972; Karp 1975a, b), and temperature gradients (Hindsley & Bell 1986).

To derive the exact phase-dependence of the p-factor, we require a full non-LTE hydrodynamic model of the Cepheid. We have used our synthetic lines computed with the time-dependent Cepheid model to measure line centers and derive radial velocities using the same techniques already applied to the observed spectral lines. This provides us with the theoretical radial velocity curve. We also have exact information, from the contribution functions, about where in the atmosphere the synthetic spectral lines were formed. Therefore, we can derive the pulsation velocity curve, as mentioned in § 3.2. Both curves are shown in Figure 10. We determine p as a function of phase from the ratio of the two curves.

The functional dependence of $p(\phi)$, reflects the basic fact that Cepheid atmospheres heat up and reduce pressure scale heights during contraction, and do the opposite during expansion. This behavior remains virtually unchanged for Cepheids of any period. The cause for the variation of p is essentially the same, as is the cause for the different line asymmetry on both sides of the velocity reversal.

More specifically, the Cepheid is hotter during expansion (i.e., the photospheric lines are formed higher) and the microturbulence is larger (after the sharp velocity reversal), which together lead to more extended CFs (in both frequency/wavelength and in depth). The spectral lines are broader and less asymmetric during expansion as a result of this, despite the fact that the mean velocity of the gas where they are formed is as high as that during contraction. Hence the larger ratio of the velocities (i.e., larger p-factor) during these phases. During contraction the Cepheid is cooler (i.e., the photospheric lines are formed deeper) and the microturbulence is lower—thus the CFs are compact and more asymmetric (the velocity gradient is seen with better "contrast"). The lines are asymmetric as expected, but they are sampling much better the velocity of the gas in the photosphere as well. Hence, p is smaller. Limb darkening has an opposite (but smaller) effect, as is visible in the left panel of Figure 10 and in a comparison of the optical (OP) and IR asymmetry curves of η Aql and ζ Gem in Figure 4. There is more limb darkening in the optical, hence there is *less* line asymmetry discrepancy between contraction and expansion phases.

Incorporating the phase-dependent p-factor into the BW technique is straightforward. The linear displacement of the atmosphere is found by integrating over the Cepheid period:

$$\int [v_r(\phi) - \gamma] p(\phi) d\phi = \int [v_r(\phi) - \gamma] \frac{v_p(\phi)}{v_r(\phi)} d\phi ,$$

where γ is the center-of-mass velocity of the Cepheid. In practice, γ is determined by demanding that the integral of the radial velocity over a whole cycle be zero (and p, normally

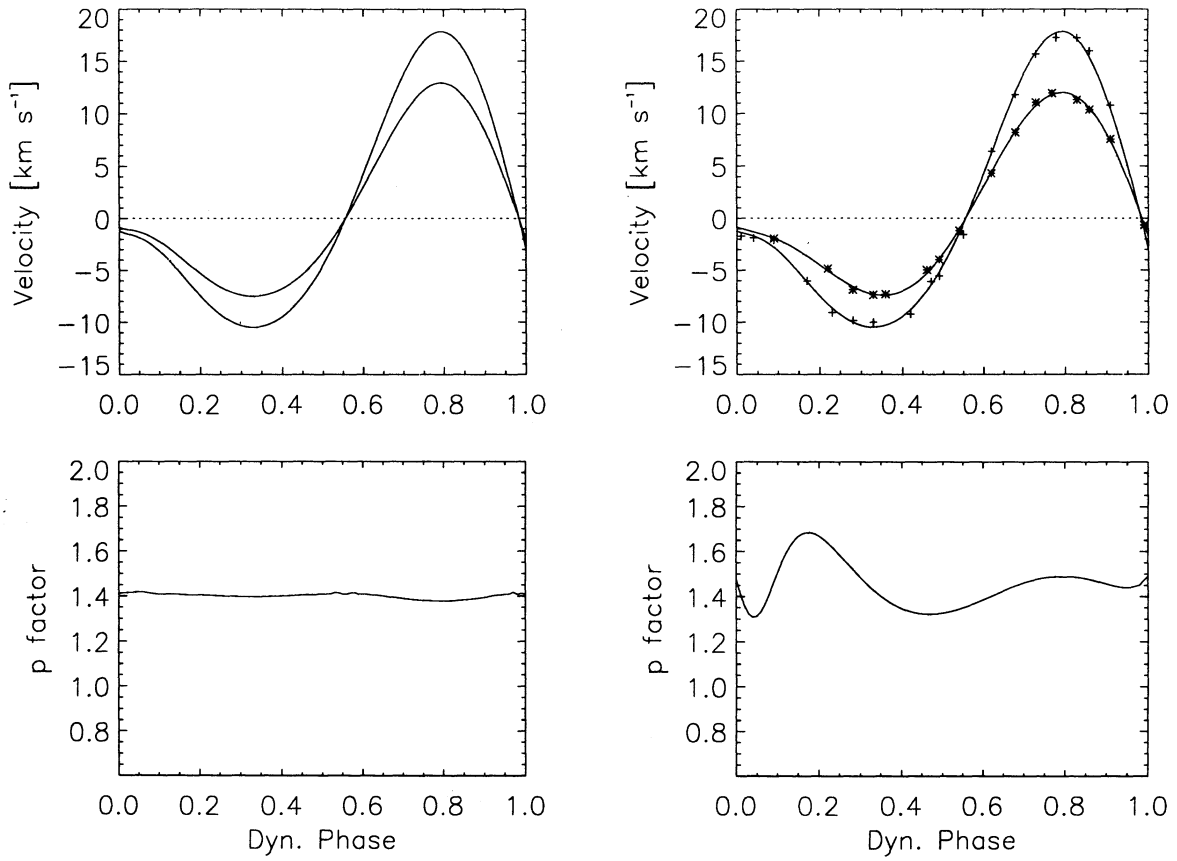

FIG. 10.—The top two panels show the theoretical pulsation velocity derived from the time-dependent model atmosphere (larger amplitude curves), and simulated observed velocity from line center measurements of theoretical absorption line profiles (smaller amplitude curves). The theoretical pulsation velocity curves are the same in both plots, but the "observed" velocity curve on the left uses a kinematic LTE line-profile calculation, while the "observed" velocity curve on the right results from the dynamic non-LTE time-dependent models. The *p*-factors which we derive from the ratio of the pulsation velocity and the measured velocity are presented in the bottom panels. The assumption of a constant *p*-factor only holds for the simple case (despite a small variation due to the varying limb darkening of the LTE model). The shape of the variable *p*-factor in the bottom right plot is explained in the text (§ 4.2).

assumed to be constant, is outside the integral), then the integration is over the radial velocity curve alone. Obviously, this is not the case in reality. Under practical circumstances one will be solving the integral

$$\int v_r'(\phi)p(\phi)d\phi \ ,$$

where $v_r'(\phi)$ is the radial velocity curve normalized to the already determined γ-velocity.

4.3. *Baade-Wesselink Radii*

The BW method for determining the mean radius of a pulsating star by combining the light and color curves with the integration of the velocity curve has been reviewed in depth by Gautschy (1987). To demonstrate the effect of using a phase-dependent *p*-factor, and different methods of measuring line center, BW radii have been calculated (Table 2 contains the results). A FORTRAN code (based on a code by Ivanov 1984) has been used, which is a standard program that gives results similar to other programs (see Burki et al. 1986, 1988). Photometry and $B-V$ intensities were taken from Moffett & Barnes (1980) and Shobbrook (1992), while constant *p*-factors were taken from Parsons (1972), and Hindsley & Bell (1986). Although the radii results are consistent with independent determinations (e.g., Fernie 1984), the purpose of calculating the BW radii was not to obtain the most accurate Cepheid radii to date (for which simultaneous photometry and spectroscopy and greater phase coverage would be essential), rather to assess the systematic effects on radii results.

As expected from the 5%–10% difference in measured velocity amplitudes between the two methods of measuring line center, the parabolic method consistently yielded larger radii by a similar factor (Table 2). In these calculations we used

TABLE 2

BAADE-WESSELINK RADII RESULTS

A. THEORETICAL

Star Name	$R/R_\odot$ $p_{const} = 1.40$	$R/R_\odot$ Using $p(\phi)$	Percent Difference
ζ Gem model (IR).....	61.4 ± 3.7	65.1 ± 3.8	6%

B. OBSERVED

Star Name	*p* Factor	$R/R_\odot$ Line Bisector	$R/R_\odot$ Parabola	Percent Difference
ζ Gem (IR)	1.40	61.8 ± 3.5	64.4 ± 3.6	4%
δ Cep (OP)	1.34	44.1 ± 6.6	46.2 ± 6.8	5
η Aql (IR)	1.43	62.7 ± 3.1	65.8 ± 3.2	5
η Aql (OP)	1.36	56.0 ± 5.1	60.4 ± 5.3	8
X Sgr (IR)	1.43	42.2 ± 4.1	66.6 ± 4.9	45

constant p-factors which correspond to the wavelength region and line bisector method of measurement. For X Sgr, the parabolic method yielded a radius more than 1.5 times as large, although the extremely discrepant X Sgr radii are a direct result of the drastic line splitting manifest in the X Sgr spectra. (Yet if our spectral resolution were not sufficient to make the splitting apparent, then this effect would still exist in a somewhat diminished form although we would no longer have line splitting to suggest caution.)

The result of using a phase-dependent p-factor, instead of a constant, was a BW radius increase of 6%. The phase-dependent p-factor was obtained from the ratio of high-order polynomial fits to the theoretical pulsation velocities (acquired using the contribution functions as described in § 3.2), and the simulated radial velocities (obtained from line bisector Doppler shift measurements of the synthetic profiles). Both velocity curves, and the phase-dependent p-factor applied, are presented in Figure 10. To be consistent, the constant p-factor used for comparison was also derived from the ratio of the model pulsation velocity to the model radial velocity, although in this case the model was simplified to a non-LTE hydrostatic calculation (like models used in the literature for that purpose). If we interpolate a constant p-factor from Parsons (1972), then we get a p-factor of 1.43 (as opposed to 1.40 from the ratio of our model velocities), yielding a 4% BW radius increase instead of 6%.

5. CONCLUSION

We have studied the influence of Cepheid atmospheric dynamics on absorption line profiles to demonstrate that measuring the pulsation velocity involves more than a straightfoward application of the Doppler principle. First, line center measurements depend systematically on the amount of line asymmetry and the method used to measure the line center. Second, the observations show that the magnitudes of the line asymmetry differ systematically between expansion and contraction stages for every Cepheid examined. The radiation hydrodynamics model reproduces these unequal line asymmetries in terms of a line-transfer effect.

In particular, we find that in the dynamic atmospheres of Cepheids the depth of line formation varies significantly with phase, that is, spectral lines do not conserve paths over a cycle. Therefore, there is a marked inequality, in terms of line formation, between the phases of Cepheid expansion and contraction. Its observational manifestation is the unequal magnitude of line asymmetries during expansion and contraction, which is now well established in a dozen Cepheids. Our simultaneous optical and infrared spectroscopy made it possible to separate the effect due to limb darkening, which is smaller.

This leads to two systematic effects in Cepheid radii and distances. First, the invalidity of path conservation demands the use of phase-dependent p-factors (for transforming between radial and pulsational velocities). Second, the line asymmetry discrepancy and invalidity of path conservation imply a systematic blueshift of the Cepheid γ-velocity. The observed magnitude of this line asymmetry discrepancy results in a γ-velocity offset of about 1 km s^{-1}, which is significant in a BW solution (at the 5% level). A systematic error in the Cepheid γ-velocities would imply systematic error in distance scale zero points determined by any method in which Cepheid velocities are used. Similarly, when included in a BW calculation, phase-dependent p-factors lead to a 5% systematic error. Both effects act in the same direction. Because the source of the effect (Cepheids atmospheres heat up during contraction) is independent of period, luminosity, or temperature (as is observed in the common line asymmetry curves), we suggest that it affects the zero point of the Cepheid distance scale by the same amount.

We suggest that an accurate reevaluation of the Cepheid scale zero point be done by deriving asymmetry curves for the sample of calibrating Cepheids. High-resolution precision spectroscopy with only moderate phase coverage can provide an asymmetry curve, which could be combined with any good radial velocity curve (with a specified method of velocity measurement) to derive a phase-dependent p-factor. Any specified method used to get the good radial velocity curve assumes zero average asymmetry over one cycle; the asymmetry curve will provide the amount and phase of the deviation from this assumption. This correction can be applied to the p-factor, via its known dependence on the method of Doppler shift measurement, as given by Parsons (1972), Karp (1975b), and Hindsley & Bell (1986) for each appropriate method. As far as determining the systematic error on the γ-velocity is concerned, model calculations need to accompany the asymmetry curve derived from high-resolution spectroscopy.

By their nature, the systematics in the line formation and velocity curves of classical Cepheids should apply to the atmospheres of other pulsating stars, most notably, the RR Lyrae variables. Offsets in the center-of-mass velocities in other types of pulsating stars may be significant as well, for example, in W Vir, RV Tau, and Mira variables.

We are grateful to the staff of McDonald Observatory and T. G. Barnes for the kind help and flexibility in scheduling the simultaneous observations. D. D. S. thanks D. Gillet, M. Breitfelner, and A. Fokin for the enlightening discussions. C. N. S. would like to acknowledge the financial support of the Theodore Dunham, Jr. Grant from the Fund for Astrophysical Research. This work was supported in part by NASA grant NAG 5-2343.

REFERENCES

Albrow, M. D., & Cottrell, P. L. 1993, South Stars, 35, 84
———. 1994, MNRAS, 267, 548
Baade, W. 1926, Astron. Nachr., 228, 359
Barnes, T., & Evans, D. 1976, MNRAS, 174, 489
Bell, R., & Rodgers, A. 1964, MNRAS, 128, 365
Breitfellner, M. G., & Gillet, D. 1994, A&A, 277, 553
Burki, G., et al. 1988, in IAU General Assembly, Baltimore
Burki, G., Schmidt, E., Arellano Ferro, A., Fernie, J. D., Sasselov, D., Simon, N., Percy, J., & Szabados, L. 1986, A&A, 168, 139
Butler, R. P. 1993, ApJ, 415, 323
Caldwell, J. A. R., & Coulson, I. M. 1987, AJ, 93, 1090
Carlsson, M. 1986, Uppsala Astron. Obs. Report 33
Carroll, J. 1928, MNRAS, 88, 548
Ciurla, T. 1966, Acta Astron., 16, 249
Coker, R., Madore, B., Mould, J., Oke, J. B., Picard, A., Huchra, J., & Latham, D. 1989, PASP, 101, 594
Davis, J. 1994, in IAU Symp. 158, Very High Angular Resolution Imaging, ed. J. G. Robertson & W. J. Tango (Dordrecht: Kluwer), 135
Fernie, J. D. 1984, ApJ, 282, 641
Gautschy, A. 1987, Vistas Astron., 30, 197
Getting, I. A. 1935, MNRAS, 95, 141
Gieren, W. P., Barnes, T. G., III, & Moffett, T. J. 1993, ApJ, 418, 135
Gustafsson, B., Bell, R. A., Eriksson, K., & Nordlund, A. 1975, A&A, 42, 407
Harris, H. C., Welch, D. L., Kraft, R. P., & Schmidt, E. G. 1987, AJ, 94, 403
Hilendahl, R. 1968, Ph.D. thesis, Univ. California at Berkeley
Hindsley, R., & Bell, R. 1986, PASP, 81, 732
Ivanov, G. 1984, Ap&SS, 105, 369
Jacoby, G., et al. 1992, PASP, 104, 599

Karp, A. 1975a, ApJ, 200, 354
———. 1975b, ApJ, 201, 641
Magain, P. 1986, A&A, 163, 135
Maillard, J., & Michel, G. 1982, in IAU Colloq. 67, Instrumentation for Astronomy with Large Optical Telescopes, ed. C. M. Humphries (Dordrecht: Kluwer), 213
Mermilliod, J. C., Mayor, M., & Burki, G. 1987, A&AS, 70, 389
Mihalas, D., & Mihalas, B. W. 1984, Foundations of Radiation Hydrodynamics (Oxford: Oxford Univ. Press)
Moffett, T., & Barnes, T. 1980, ApJS, 44, 427
Parenago, P. P. 1947, Var. Stars (USSR), 6, 102
Parsons, S. B. 1972, ApJ, 174, 57
Pont, F., Mayor, M., & Burki, G. 1994, A&A, 285, 415
Sanford, R. 1956, ApJ, 123, 201
Sasselov, D. D., & Lester, J. B. 1990, ApJ, 362, 333
———. 1994, ApJ, 423, 795
Sasselov, D. D., & Raga, A. 1992, in Cool Stars, Stellar Systems, and the Sun (ASP Conf. Series 26), 549
Schwarzschild, M., Schwarzschild, B., & Adams, W. 1948, ApJ, 108, 207
Shapley, H., & Nicholson, S. B. 1919, Proc. Natl. Acad. Sci., 5, 417
Shobbrook, R. R. 1992, MNRAS, 255, 486
Stibbs, D. W. N. 1956, MNRAS, 116, 453
Underhill, A. B. 1947, ApJ, 106, 128
Van Hoof, A., & Deurinck, R. 1952, ApJ, 115, 166
Van Paradijs, J. 1971, A&A, 11, 299
Walker, A. 1988, in The Extragalactic Distance Scale (ASP Conf. Series 4), 89
Wallerstein, G., Jacobsen, T., Cottrell, P., Clark, M., & Albrow, M. 1992, MNRAS, 259, 474
Welch, D. L. 1994, AJ, 108, 1421
Wesselink, A. 1946, Bull. Astron. Inst. Netherlands, 10, 91
Wielen, R. 1974, A&AS, 15, 1
Willson, L. A. 1988, in A Decade of UV Astronomy with IUE, ESA SP-281, 29
Wilson, O. C. 1935, ApJ, 82, 233
Wilson, T. D., Barnes, T. G., Hawley, S. L., & Jefferys, W. H. 1991, ApJ, 378, 708